Engineering Structures 288 (2023) 116198

Contents lists available at ScienceDirect

Engineering Structures

journal homepage: www.elsevier.com/locate/engstruct

Eurocode-compliant system safety factor for advanced design of hollow section Warren trusses

Lauri Jaamala [a,*], Kristo Mela [a], Juha Tulonen [b], Anssi Hyvärinen [b]

[a] Tampere University, Tekniikankatu 12, 33720 Tampere, Finland
[b] SSAB, Harvialantie 420, Hämeenlinna 13300, Finland

ARTICLE INFO

Keywords:
Reliability study
Structural system
Cold-formed
High-strength steel
Advanced design method
Direct design method
Warren truss

ABSTRACT

Eurocode allows for the design of structural systems by advanced analysis, i.e. by **G**eometrically and **M**aterially **N**onlinear **I**mperfection **A**nalysis (GMNIA). In GMNIA, the entire structural system is designed by carrying out a nonlinear finite element analysis and by comparing the load proportionality factor obtained from the analysis to the predetermined system safety factor. This study determines the required Eurocode-compliant GMNIA system safety factor for the ultimate limit state design of Warren-type roof trusses. The system safety factor is determined based on system-level reliability studies conducted for 15 trusses. The investigated trusses are made of cold-formed rectangular hollow sections having a nominal yield strength of 700 MPa. The determined system safety factor is then applied for comparison calculations, in which three trusses are designed both by GMNIA and the conventional EN 1993-1-1 method. This comparison reveals a need for an accurate modelling method of hollow section connections in GMNIA. Furthermore, the comparison shows that GMNIA can offer reduced material consumption compared to the conventional method even in roof trusses, in which load redistribution capabilities are very limited. This reduction is achieved due to capability of GMNIA to accurately capture the buckling capacities of continuous top chords, whereas the conventional method must rely on conservative approximations of buckling lengths.

1. Introduction

Modern desktop computers and commercial Finite Element Method (FEM) packages can carry out geometrically and materially nonlinear finite element analyses (NFEA) even for large structural systems. Eurocode 3 [1,2] permits the utilization of NFEA in design and this type of Advanced Design Method (ADM) is termed GMNIA, which stands for **G**eometrically and **M**aterially **N**onlinear **I**mperfection **A**nalysis. ADMs harness the full computational power of modern computers for design use. This can lead to improved material efficiency of structures compared to conventional member-based design methods because material plasticity and redistribution of forces can be accounted for in a complete structural system [3–5]. In addition, ADM offers a comprehensive understanding of the collapse mode of structural systems and leads to more uniform system reliability compared to conventional member-based design methods [6], hence increasing the safety of the design. In ADM, the entire structural system, e.g. a steel frame, can be designed by using the formula [5]:

$$\frac{R_n}{\gamma_{ADM}} \geq \sum \gamma_i \bullet Q_{ki} \tag{1}$$

where R_n is the nominal ultimate strength of the structural system determined by advanced analysis (e.g., NFEA) using the nominal geometric and material properties including the effects of imperfections, γ_{ADM} is a system safety factor that considers the uncertainties that affect the strength of the structural system, and Q_{ki} and γ_i are the characteristic loads (gravity, wind loads) and partial factors for actions in load combinations, respectively, according to the relevant standards (e.g., Eurocode 1 [7] and Eurocode 0 [8]). The nominal ultimate strength R_n is determined by static structural analysis, where the applied loads are scaled up incrementally by the load factor α. The ultimate load factor, α_u, is determined as the highest load factor in the load–displacement curve of the system or as the highest load factor for which the largest strain in structural members is within allowable limits. Additionally, α_u may be determined at the point in which the stiffness of the structure has been reduced e.g. to 5 % from the initial stiffness determined from the load–displacement curve [5]. The ultimate load factor represents the

* Corresponding author.
E-mail address: lauri.jaamala@tuni.fi (L. Jaamala).

https://doi.org/10.1016/j.engstruct.2023.116198
Received 6 February 2023; Received in revised form 14 April 2023; Accepted 18 April 2023
Available online 11 May 2023

ratio between the nominal resistance and applied loads, hence Eq. (1) can be reformulated as $\alpha_u \geq \gamma_{ADM}$ [5].

Unfortunately, despite the advantages, the design by GMNIA has not been widely adopted in practice. This may be explained by the following three observations. Firstly, utilizing GMNIA requires expert knowledge in considering the effects of various imperfections, such as the effects of residual stresses, in the calculation model. EN 1993 offers a simple method, "Equivalent geometrical imperfections" (EGI), by which the various imperfections can be considered in the model by the global geometrical bow imperfection in the sinusoidal shape δ_1 as shown in Fig. 1. However, a fixed magnitude for EGI can not consider the effects of residual stresses accurately for various member slendernesses [9,10], and no other guidance has been given in EN 1993 to model the residual stresses. Fortunately, a recent study [10] validated the so-called "effective material model" (EMM) that enables an accurate and simple way of incorporating residual stresses in beam element-based GMNIA models. The EMM is based on modifying the (nonlinear) stress–strain curve to account for the effects of residual stresses.

Secondly, in GMNIA, the so-called model uncertainty factor α_1 needs to be determined with the conventional Eurocode partial factor for resistance γ_M to obtain γ_{ADM} [2]:

$$\gamma_{ADM} = \gamma_M \bullet \alpha_1 \tag{2}$$

Determining α_1 requires FEM model calibrations against experimental capacity test results. Therefore, this procedure seems suitable for manufacturers of isolated structural products, which can use the "design assisted by testing" procedure presented in EN 1990 [8]. For a designer of a general structural system, however, determining the α_1 may be impossible because of the lack of available test results.

The third observation is that the γ_M value in Eq. (2) is selected according to the relevant failure mode from partial factors of γ_{M0}, γ_{M1}, or γ_{M2} [2,11], which may lead to various γ_{ADM} values. This is problematic for such structural systems in which the governing failure mode is not evident. Consider for example a roof truss, for which e.g. $\gamma_{ADM} = 1.15$ for buckling and $\gamma_{ADM} = 1.2$ for tensile fracture have been derived. The truss must provide $\alpha_u \geq 1.2$ to ensure sufficient tensile capacity. It may happen during the analysis that a member buckles for $1.15 < \alpha_u < 1.2$. If the structure fails after $\alpha_u = 1.15$ but before $\alpha_u = 1.2$, then the buckling capacity is verified but the tensile capacity, e.g. resistance of a bottom chord, is not. This means basically that the system resistance must be verified against the most demanding γ_{ADM} leading to an over-conservative design for failure modes which require smaller γ_{ADM}.

Based on the above observations, a practical GMNIA procedure requires clear guidance in generating a proper FEM model and a single system safety factor that does not need access to experimental test results. Consequently, the design outcome of GMNIA will become harmonized and safe among practitioners. Currently, a new Eurocode EN 1993-1-14 [11], "Design assisted by finite element analysis", is under development. This standard is a great improvement to the current situation regarding the guidance of performing the design by GMNIA. However, EN 1993-1-14 still requires test results for calculating the model uncertainty α_1, denoted as model factor γ_{FE} in EN 1993-1-14, thus complicating the determination of γ_{ADM} for structures from which experimental test results cannot be found.

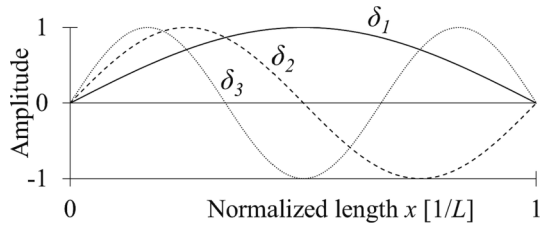

Fig. 1. Sinusoidal shapes δ_1, δ_2 and δ_3 for geometrical imperfections e_1, e_2 and e_3, respectively.

This study develops a practical GMNIA procedure for cold-formed rectangular hollow section (CFRHS) structures that solves the above-mentioned difficulties. The hollow sections are made of steel grade S700 and fabricated by the continuous forming method [12]. For these sections, the corner regions have higher material strength compared to flat regions, and additionally, high residual stresses exist in the longitudinal and transverse directions. The studied structural systems are planar Warren roof trusses, i.e. K-jointed trusses, in which CFRHS are widely used. Fig. 2 presents three layouts in scale, which are used in the development of the Eurocode-compliant GMNIA procedure for the ultimate limit state design. The procedure is based on the "Advanced Analysis" -method of Australian and New Zealand standard AS/NZS 4600 [13] (also called Direct Design Method in the literature), in which the aforementioned experimental tests have been substituted by conducting reliability studies for prequalified structural systems [5,14–16]. In reliability studies, numerical tests in the form of Monte Carlo simulations (MCS) are carried out to determine statistical distributions of resistances of structural systems, from which the required system safety factors can be derived [17]. The present study determines these system safety factors and additionally proposes principles for generating nominal models which are to be used by practitioners. Finally, three Warren trusses are designed by the developed approach and results are compared with the conventional member-based design method. This comparison reveals the need for further research but also indicates that the design by GMNIA can result in more economical material consumption than the conventional method even in truss structures in which load redistribution capabilities are very limited.

2. Modelling cold-formed hollow sections

An accurate NFEA model is required for ADM that considers the effects of material properties and governing imperfections in structural members. Only a brief description regarding these properties is given in this section, and more detailed presentations are provided for residual stresses in [18] and for material properties and effective material model (EMM) in [10].

2.1. Material properties and residual stresses

Table 1 presents material properties employed for S700 CFRHS regarding the flat region. Except for the elastic modulus, Poisson's ratio and density, these parameters were determined based on the dataset obtained from the manufacturer of CFRHS (DSet). It should be noted that the mean stress values f_y, f_u and $\sigma_{0.05}$ presented in Table 1 are the mean production test values multiplied by a factor of 0.9965 for considering the strain rate effects [10,19]. The corner material is assumed to extend by the distance of $2t$ into the flat region, where t is the wall thickness of the cross-section, see Fig. 3 [20–24]. Tables 2 and 3 present corner strength enhancement factors and material properties for the corner regions, respectively. It should be noted that corner strength enhancement factors are based on only 12 measured values. Therefore, C_{fy} has been truncated based on measured lower and upper bound values, into the interval [1.06, 1.34], to prevent unrealistically high or low C_{fy} factors.

A two-stage Ramberg-Osgood model [27] is used to model the stress–strain curves up to f_u. For the flat material, at f_u, a constant yield plateau remains up to the strain of 5 %, after which the stress decreases linearly to the level of 3/4 of f_u at strain 10 %, see Fig. 4. The stress decrease in the material model accounts for the necking phenomenon, which is not explicitly modelled in beam elements. For the corner material, a constant yield plateau having a length of 0.1 % strain is assumed after ε_u, and then a linear stress decrease to 3/5 of f_u is assumed at strain 10 % [10].

CFRHS have bending residual stresses in the longitudinal and transversal directions. These stresses vary along the perimeter of the section and nonlinearly through the thickness of the material [10].

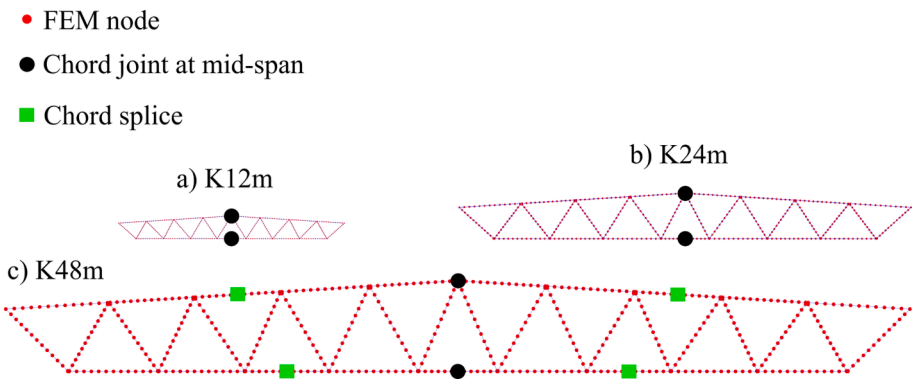

Fig. 2. Base geometries and element meshes of K-trusses.

Table 1
Material properties for the flat region of the steel grade S700.

Property	Description	Distribution	Mean μ	CoV [%]	Nominal value	Ref.
f_y	Yield strength	Normal	746.5 MPa	2.76	700.0 MPa	DSet
f_u	Ultimate strength	Normal	839.5 MPa	2.47	750.0 MPa	DSet
$\sigma_{0.05}$	0.05 % proof stress	Normal	641.9 MPa	5.47	586.4 MPa	DSet
ε_u	Strain at f_u	Normal	0.037	25.18	0.037	DSet
E	Elastic modulus	Normal	210 GPa	3.00	200 GPa	[25,26]
ν	Poisson's ratio	Deterministic	0.3	–	0.3	[1]
ρ	Density	Deterministic	7850 kg/m^3	–	7850 kg/m^3	[7]

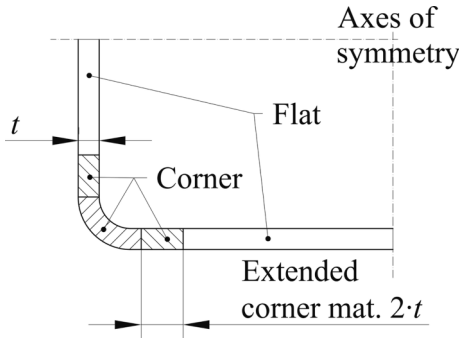

Fig. 3. Material regions Flat and Corner presented for 1/4th of the cross-section.

Table 2
Corner strength enhancement factors of the steel grade S700 [10].

Property	Description	Distribution	Mean μ	CoV [%]	Nominal value
C_{fy}	Corner strength enhancement factor for f_y and $\sigma_{0.05}$	Student's t (n = 12)	1.21	6.74	1.21
C_{fu}	Corner strength enhancement factor for f_u	Full correlation with C_{fy}	$C_{fu} = 0.346 \bullet C_{fy} + 0.743$		1.16

Table 3
Material parameters for the corner regions of the steel grade S700 [10].

Property	Mean and Nominal
f_y	$C_{fy} \bullet f_y$ of the flat region
f_u	$C_{fu} \bullet f_u$ of the flat region
$\sigma_{0.05}$	$C_{fy} \bullet \sigma_{0.05}$ of the flat region
ε_u	1.7% (full correlation with the flat)
E, ν, ρ	E, ν, ρ of the flat region

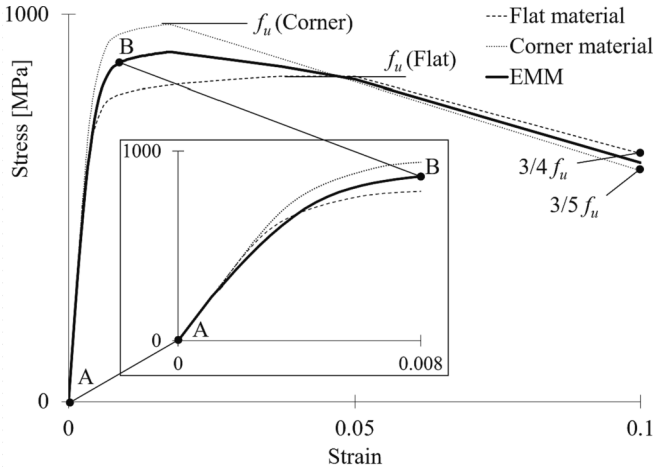

Fig. 4. The mean stress–strain curves of the flat and corner and the EMM illustrated for CFRHS 120×120×8 S700.

Table 4 presents the statistical properties of residual stress components. This study utilizes the residual stress model of Jaamala et al. [18] in modelling residual stresses with two exceptions: (1) Longitudinal bending residual stresses have been multiplied by the factor of 0.7 to exclude the 30 % portion of residual stresses that have been inherently included to the measured stress–strain curves of the base materials flat and corner [10]; (2) Probabilistic distribution for transversal residual stresses has been truncated to 0 in the case of sampled negative values: The sampled values below zero are rare, hence this has a negligible or slightly conservative effect on buckling capacities because negative transversal residual stress distribution can be beneficial for the member [18]. Correlations were found between some of the variables and their correlation coefficients are presented in Tables 5 and 6.

2.2. Effective material model

General purpose beam elements of commercial FEM packages have

Table 4
Statistical distributions for geometrical properties, residual stresses, and modelling uncertainty.

Property	Description	Distribution	Parameters[1]	Nominal value	Ref.
W	Width	Normal	$\mu = 1.00$, $\sigma = 3.17e{-}3$ [$1/W_{Nominal}$]	1.0	DSet
H	Height	Normal	$\mu = 1.00$, $\sigma = 3.17e{-}3$ [$1/H_{Nominal}$]	1.0	DSet
t	Thickness	Generalized extreme value	$\mu = 0.9824$, $\sigma = 1.24e{-}2$, $\xi = 4.60e{-}2$ [$1/t_{Nominal}$]	1.0	DSet
e_1	1. bow imperf.	Normal	$\mu = 0.0$, $\sigma = 2.458e{-}4$ [$1/L$]	L_{FS}/1000	[23,28,29,5]
e_2	2. bow imperf.	Normal	$\mu = 0.0$, $\sigma = 7.374e{-}5$ [$1/L$]	NA	[23,28,29,5]
e_3	3. bow imperf.	Normal	$\mu = 0.0$, $\sigma = 4.424e{-}5$ [$1/L$]	NA	[23,28,29,5]
$\sigma_{LB,Flat}$	Longit. residual stress in flat	Normal	$\mu = 0.70 \bullet [-7.694e{-}7\, f_y^2 + 6.737e{-}4\, f_y + 0.562]$, $\sigma = 0.206$ [$1/f_y$]	μ	[10,18]
$\sigma_{LB,Corner}$	Longit. residual stress in corner	Normal	$\mu = 0.70 \bullet [-4.757e{-}7 f_y^2 + 2.161e{-}4\, f_y + 0.548]$, $\sigma = 0.196$ [$1/f_y$]	μ	[10,18]
$\sigma_{TB,Flat}$	Trans. residual stress in flat and corner	Normal	$\mu = -2.339e{-}7\, f_y^2 + 7.613e{-}5\, f_y + 0.324$, $\sigma = 0.155$ [$1/f_y$]	μ	[10,18]
θ_M	Modelling uncertainty	Lognormal	$\mu = 1.0$, $\sigma = 0.05$	NA	[5]

[1] μ = mean and σ = standard deviation for Normal and Lognormal distributions, μ = location, σ = scale and ξ = shape for Generalized extreme value distribution.

Table 5
Correlation coefficients for material parameters [DSet].

	f_y	f_u	$\sigma_{0.05}$
f_y	1.0	0.70	0.70
f_u	symm.	1.0	0.0
$\sigma_{0.05}$	symm.	symm.	1.0

Table 6
Correlation coefficients for residual stress components [18].

	$\sigma_{LB,Flat}$	$\sigma_{LB,Corner}$	$\sigma_{TB,Flat}$
$\sigma_{LB,Flat}$	1.0	0.80	0.76
$\sigma_{LB,Corner}$	symm.	1.0	0.69
$\sigma_{TB,Flat}$	symm.	symm.	1.0

usually only one integration point in the thickness direction in hollow sections such that they are not capable of modelling the varying residual stress field through the material thickness. Therefore, this study employs an approximation method, the so-called "Effective material model" (EMM) [10], in which residual stresses are considered by reducing the stress–strain curve of the material. EMM also considers the corner strength enhancement by composing the stress–strain curve as a weighted average from the flat and corner region materials. Fig. 4 illustrates the EMM for a CFRHS 120×120×8 with the mean material and residual stress properties. The separate curve inside the figure, which is rescaled into the interval [A,B], shows how the initial stiffness, i.e. the slope of the linear part of the curve, has been reduced in the EMM compared to base materials flat and corner. This reduction is due to the effects of residual stresses. Fig. 4 also shows how the ultimate stress of the EMM is about the average of the f_u's of the flat and corner materials because both flat and corner regions constitute about half of the cross-section 120×120×8. It should be noted that the base materials "flat" and "corner" are used only in generating the EMMs, and in GMNIA analysis, the EMMs are applied as the stress–strain curves for the beam elements. Additionally, because the material and geometrical properties and magnitude of residual stresses are random variables in reliability studies, and because the EMM is dependent on the relative areas of flat and corner materials in a cross-section, every structural member has a unique EMM. Hence, the stress–strain curves of members are both material but also cross-sectional properties.

2.3. Geometrical properties

Cross-sectional dimensions and member straightness are considered as random variables, whose distributions and properties are given in Table 4. Bow imperfections are modelled by using three sinusoidal modes $i = 1\ldots3$ according to the equation:

$$e_{tot}(x) = \sum e_i \bullet \sin(i\pi x) = \sum e_i \bullet \delta_i(x) \tag{3}$$

in which $x \in [0,1]$ is a normalized coordinate along the member length, e_i is the bow magnitude of the i:th mode, and δ_i is the sinusoidal shape as presented in Fig. 1. Statistics for e_1 were determined based on 127 maximum bow measurements found from studies [23,28,29], excluding member lengths below 500 mm from the study [29]. Magnitudes for e_2 and e_3 were determined based on the relation that e_2 is about 30 % of e_1 and e_3 about 18 % of e_1 [5]. Actual bow imperfection is obtained by multiplying e_{tot} with the span length of the member, L, as shown in Table 4. Bow imperfections are modelled in 3D independently in both cross-sectional directions of the member.

3. Warren trusses

In this study, the system safety factor γ_{ADM} is determined for a class of planar roof trusses based on a total of 15 various Warren truss configurations. These configurations consider three various span lengths, i.e. base geometries, which are presented in Fig. 2 and Table 7. Fig. 5 presents the naming convention of the truss dimensions. Heights at mid-span, H_m, are selected as 1/10 of the span lengths according to the recommendation in [30]. Height at supports, H_s, are determined such that the roof slope ratio is 1:16 which is common in industrial buildings. In every truss, it is assumed that top chords (TC) are restrained in the Y-axis (out-of-plane) direction (see Fig. 5) with roofing such that top chords can buckle only in the XZ plane. All translations are fixed at support A, whereas at support B, only translations in Y- and Z-directions are fixed.

Table 7
Base geometries of trusses K12m, K24m and K48m.

Truss	L_s [m]	H_s [m]	H_m [m]	Num. of braces	TC_1; TC_2; TC_3; TC_4 [m]	BC_1; BC_2; BC_3; BC_4 [m]
K12m	12	0.825	1.20	16	1.5; 1.5; 1.6; 1.5	1.5; 1.4; 1.4; 0.8
K24m	24	1.650	2.40	16	3.3; 2.9; 2.9; 2.9	3.0; 2.8; 3.1; 1.3
K48m	48	3.300	4.80	20	5.5; 4.5; 4.6; 4.7; 4.7	4.8; 4.6; 4.5; 4.7; 2.1

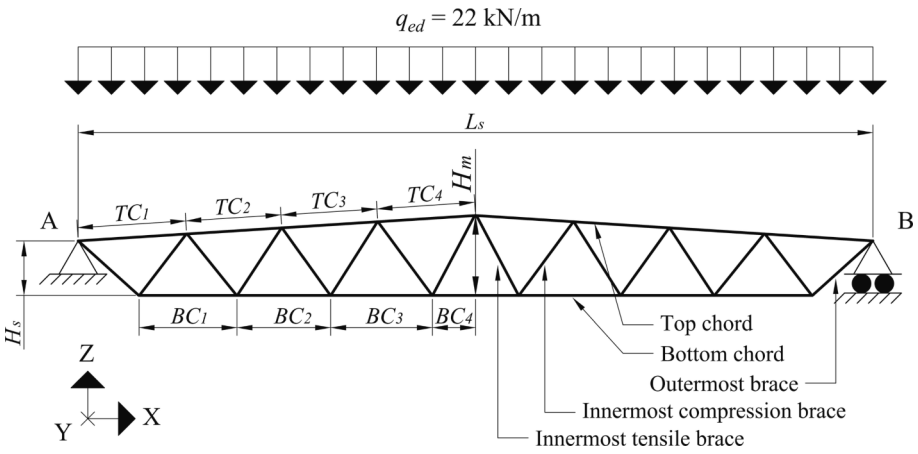

Fig. 5. Naming convention of the truss geometry and loads and boundary conditions.

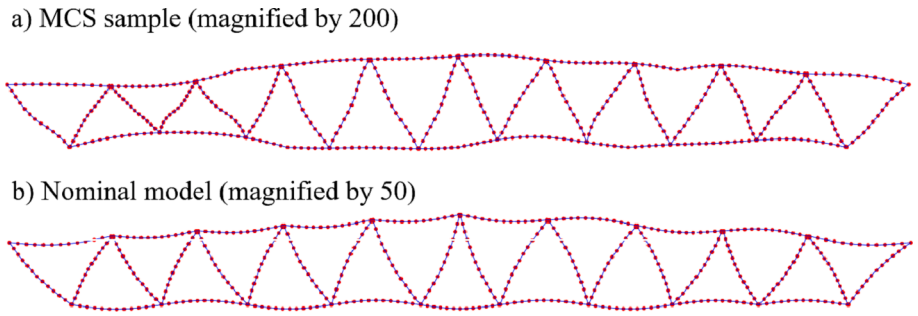

Fig. 6. Geometrical imperfections in the XZ-plane in one of the MCS samples (a) and nominal models (b) of K48mF1.

Typically, the maximum length of cold-formed hollow sections is 12–18 m. Therefore, the chords of the largest truss K48m are assumed to be constructed by joining 2 separate hollow sections per the left and right chords, see chord splices in Fig. 2. Considering two members per chord ensures that imperfections in reliability studies are properly modelled. Bow imperfections (with 200-fold magnification) for one of the MCS samples of K48mF1 are shown in XZ-plane in Fig. 6 (a), illustrating the discontinuity in bow imperfections caused by chord splices. Chord joints at mid-span (see Fig. 2), and additionally chord splices of K48m, are assumed to be rigid such that forces and moments are transferred along the chord members. However, connections between braces and chords are assumed as pinned such that only forces are transferred. Trusses shown in Fig. 2 are symmetrical with respect to the mid-span, thus only configurations for half of the trusses are shown in the following tables.

In this study, truss configurations are designed for a line load q_{ed} = 22 kN/m on the top chord (see Fig. 5) and for the self-weight of the CFRHS members. The line load is assumed to consist of permanent (0.5 kN/m^2) and snow loads (2 kN/m^2) on the roof with the truss spacing of 6 m and by applying the partial factors $\gamma_G = 1.35$ for the permanent load (and for self-weight) and $\gamma_Q = 1.50$ for snow load according to Eurocode 0 [8].

Various failure modes can occur in trusses such as buckling in the top chord or the compressed brace or tensile fracture in the bottom chord or tensioned brace. These failure modes must be considered in the system safety factor. Therefore, Table 8 presents five various truss configurations, F1–F5, for every base geometry. Member profiles are chosen from a catalogue provided for S420 and here also employed for S700 [31]. For each member, the smallest (lightest) profile is chosen for which the design rules of EN 1993-1-1 are satisfied. Compressed members are limited to cross-section classes 1 or 2 having the maximum Eurocode 3 non-dimensional slenderness $\bar{\lambda} \leq 3.0$. The non-dimensional slenderness limit affects mostly the selection of the innermost compression braces in the mid-span (see Fig. 5), in which the axial forces are small. Without a such limit on the slenderness, these members would become extremely thin. Additionally, the minimum material thickness of members is 3 mm and the minimum width of chords is limited to the width of the largest brace such that joints are practicable. Buckling lengths of chords are assumed to be 0.9 times the system lengths and buckling lengths of braces as the full system lengths even the reduced lengths for braces could be used in welded connections [1].

The truss configurations F1–F5 of Table 8 have been designed such that in F1, the target utilization ratios (maximum allowed utilization ratios) based on conventional EN 1993-1-1 design are 1.0 for all members. In F2–F5, however, target utilization ratios have been set such that for members which are desired to fail, the target utilization ratio is kept at 1.0 and for the rest of the truss members the target ratio is set to 0.7. This arrangement ensures that various failure modes are studied, but naturally, does not guarantee that the desired member fails in every sample of reliability studies. The desired failure members are bottom chords in F2, top chords in F3, tension braces in F4, and compression braces in F5.

4. Finite element model

Structural analyses are carried out by the Abaqus software [32] using Abaqus beam elements of type B31. The cross-section is modelled with the Abaqus "ARBITRARY" definition, which enables the modelling of rounded corners by five integration points per the corner arc. According to mesh convergence studies, mesh size was chosen such that every structural member between truss joints was modelled using 12 elements. This element division allows for accurate modelling of the three imperfection modes e_1, e_2 and e_3 (see Fig. 1). Bow imperfections are considered independently in both XZ- and YZ-planes. Fig. 2 presents the

Table 8
Cross-sections of K-trusses in the reliability studies.

Truss	Top chord Bottom chord	Braces from support to mid-span
K12mF1	80×80×4.0 30×50×4.0	25×25×3.0; 50×50×3.0; 25×25×3.0; 40×40×3.0; 25×25×3.0; 40×30×3.0; 25 ×25×3.0; 25×25×3.0
K12mF2	90×90×4.0 40×60×3.0	40×30×3.0; 60×60×3.0; 25×25×3.0; 50×50×3.0; 25×25×3.0; 40×40×3.0; 25 ×25×3.0; 25×25×3.0
K12mF3	80×80×4.0 40×60×4.0	40×30×3.0; 60×60×3.0; 25×25×3.0; 50×50×3.0; 25×25×3.0; 40×40×3.0; 25 ×25×3.0; 25×25×3.0
K12mF4	90×90×4.0 40×60×4.0	25×25×3.0; 60×60×3.0; 25×25×3.0; 50×50×3.0; 25×25×3.0; 40×40×3.0; 25 ×25×3.0; 25×25×3.0
K12mF5	90×90×4.0 50×50×4.0	40×30×3.0; 50×50×3.0; 25×25×3.0; 40×40×3.0; 25×25×3.0; 40×30×3.0; 25 ×25×3.0; 25×25×3.0
K24mF1	120×120×5.6 50×90×4.0	40×40×4.0; 90×90×4.0; 25×25×3.0; 70×70×4.0; 25×25×3.0; 60×60×3.0; 50×50×3.0; 25×25×3.0
K24mF2	140×140×5.6 40×100×4.0	60×60×3.0; 100×100×4.0; 40×30×3.0; 80×80×4.0; 25×25×3.0; 70×70×3.0; 50×50×3.0; 25×25×3.0
K24mF3	120×120×5.6 60×100×5.0	60×60×3.0; 100×100×4.0; 40×30×3.0; 80×80×4.0; 25×25×3.0; 70×70×3.0; 50×50×3.0; 25×25×3.0
K24mF4	140×140×5.6 60×100×5.0	40×40×4.0; 100×100×4.0; 25×25×3.0; 80×80×4.0; 25×25×3.0; 70×70×3.0; 50×50×3.0; 25×25×3.0
K24mF5	140×140×5.6 60×100×5.0	60×60×3.0; 90×90×4.0; 40×30×3.0; 70×70×4.0; 25×25×3.0; 60×60×3.0; 50×50×3.0; 25×25×3.0
K48mF1	180×180×8.0 60×140×6.0	70×70×4.0; 140×140×5.6; 40×40×4.0; 120×120×5.0; 30×30×3.0; 110×110×5.0; 25×25×3.0; 90×90×4.0; 90×90×4.0; 25×25×3.0
K48mF2	200×200×8.8 50×150×6.0	90×90×4.0; 150×150×6.0; 70×70×3.0; 140×140×5.6; 40×40×4.0; 120×120×5.0; 25×25×3.0; 90×90×4.0; 90×90×4.0; 25×25×3.0
K48mF3	180×180×8.0 80×160×7.1	90×90×4.0; 150×150×6.0; 70×70×3.0; 140×140×5.6; 40×40×4.0; 120×120×5.0; 25×25×3.0; 90×90×4.0; 90×90×4.0; 25×25×3.0
K48mF4	200×200×8.8 80×160×7.1	70×70×4.0; 150×150×6.0; 40×40×4.0; 140×140×5.6; 30×30×3.0; 120×120×5.0; 25×25×3.0; 90×90×4.0; 90×90×4.0; 25×25×3.0
K48mF5	200×200×8.8 140×140×5.6	90×90×4.0; 140×140×5.6; 70×70×3.0; 120×120×5.0; 40×40×4.0; 110×110×5.0; 25×25×3.0; 90×90×4.0; 90×90×4.0; 25×25×3.0

mesh density of trusses and Fig. 6 (a) the magnified bow imperfections in the XZ-plane for one of the samples of the case K48mF1.

Eccentricities in brace-to-chord connections have been considered by modelling the ends of braces to the actual locations on the surface of chords, and by connecting the brace ends to chord centerlines with Abaqus "beam" type multipoint constraints (MPC). Pinned brace connections are achieved by releasing rotational degrees of freedom (DOF) about both local bending axes from brace ends while keeping torsional DOF fixed. The prescribed modelling method applies for every other joint but not for the outermost braces (see Fig. 5), from which the bending DOF is not released in the YZ-plane. This ensures a slight stiffness for the bottom chord and braces in the Y-axis direction preventing the truss to become a mechanism. The outermost braces are in tension, hence fixing the bending DOF in YZ-plane has an insignificant effect on their capacity. Additionally, because the joint of the outermost brace and top chord has no joint eccentricity due to a single connecting brace, the outermost brace is connected directly to the top chord centerline without MPC.

EMM is employed for material modelling for all members. The material is modelled according to von Mises yield surface and associated plastic flow with isotropic hardening. The analysis is performed by the arc-length method with force-controlled loading.

The authors have not found any experimental tests conducted for whole structural systems made of S700 CFRHS. However, the FEM model was validated against 30 experimental isolated column buckling tests [10] and a close correspondence to the reality was obtained. Additionally, the used software and element type have been successfully employed elsewhere [33] for analyzing entire truss structures fabricated from hot-finished hollow sections and loaded until failure, thus illustrating the sufficient accuracy of the used procedure. In reliability studies, the modelling uncertainty θ_M is considered according to the properties presented in Table 4.

5. Nominal model

The nominal model is the NFEA model which is used by the design engineer in determining the nominal resistance R_n of the structural system, see Eq. (1). Nominal parameters can be selected in various ways, but often the 5 % fractile values or minimum guaranteed values based on product standards are chosen for nominal strength parameters. The more conservative selection of nominal parameters, e.g. lower nominal f_y, results in lower nominal resistance and in higher mean-to-nominal ratio in the reliability study. Consequently, the higher mean-to-nominal ratio results in lower system safety factor. Therefore, the selected nominal parameters and obtained system safety factor are dependent on each other, and this has to be taken into account when choosing which nominal values are employed.

As discussed in Section 1, the current GMNIA procedure may lead to various γ_{ADM}-values depending on the failure mode, which further results in overconservative design. This study derives a single γ_{ADM}-value for both the instability and tensile fracture. Therefore, nominal models must provide safety factors which are approximately equal for both studied failure modes such that the selection of a single system safety factor among the derived ones leads to an acceptable low variation in reliability level. Tables 1–4 present the selected nominal parameters and it was found in this study that these parameters led to rather uniform reliability levels among buckling and tensile failures. Nominal values of f_y and f_u are selected according to the nominal values of EN 1993-1-12 [34]. Nominal values for $\sigma_{0.05}$ and E have been chosen as characteristic 5 % fractile values and geometrical properties of cross-sections as nominal values from product standards [1,8,26]. Strain ε_u and residual stresses are according to the mean values [2].

The usual practice in introducing geometrical bow imperfections to the nominal model is to superimpose the scaled elastic buckling modes [35]. According to Arrayago and Rasmussen [36], the lowest ultimate resistance of the steel frame is found accurately enough by combining the 6 lowest buckling modes with positive amplitudes. In the case of trusses, however, the lowest buckling modes may not cause imperfections for every brace, or the magnitude may become less than $L/1000$ because the scaled magnitude is related to the most imperfect member in the mode. Therefore, this study neglects eigenmodes and applies a sinusoidal mode e_1 with a magnitude of $L_{FS}/1000$ for every free span L_{FS} by offsetting nodes with the Python program. Free spans of braces are member lengths L. In chords, however, they are the spans limited by the brace connections or chord joints at mid-span, but not spans limited by the chord splices in K48m. The nominal magnitude of $L_{FS}/1000$ [11] covers, to some extent, both the bow imperfection and load eccentricities [37]. Fig. 6 (b) illustrates these nominal bow imperfections in XZ-plane for truss K48mF1.

Resistance of the nominal model corresponds to a particular combination of bow imperfection directions that yields the minimum resistance for the structure [11], and determining this combination is not evident in general. As design by GMNIA may involve hundreds of nominal analyses per structural system when feasible or optimum configuration is sought, it would be desirable that the nominal resistance would be found in practice by analyzing only a few bow imperfection directions per load case.

In this study, it is assumed that the lowest nominal resistance is found by analyzing a total of 66 nominal models per truss configuration. The number of nominal analyses was chosen somewhat arbitrarily with the assumption that 66 analyses would cover the range of imperfection combinations sufficiently. These analyses differ from each other such that bow directions in XZ-, YZ- and 3D -planes are modelled for 22 of the 66 analyses in each direction. Bow imperfections in the 3D plane are modelled as a magnitude of $L_{FS}/1000$ in the diagonal direction, i.e. as a magnitude of $\sin(45°)\bullet L_{FS}/1000$ in XZ- and YZ-directions. Among these 22 analyses per direction, a randomly generated bow direction pattern is

applied for every member in 20 of the analyses. Additionally, the remaining two analyses per XZ-, YZ- and 3D-planes have positive and negative bow directions according to local beam element directions to verify that both directions are tested for every member. The minimum resistance among these six analyses consisting of only positive or negative bow directions in XZ-, YZ- and 3D-planes is nominated as $R_{n\pm}$, whereas the actual nominal resistance R_n is the minimum of all 66 nominal analyses. The above procedure aims to study the sensitivity of the bow directions to the nominal resistance. The most desired outcome is that the nominal resistance R_n has a close correspondence to $R_{n\pm}$ such that only a few nominal models must be studied in practical applications to find the lowest resistance.

6. Reliability procedure

Reliability analysis is a powerful tool for code calibration enabling the determination of theoretical failure probabilities and required safety factors for structural systems [17]. The probability of failure can be determined by $P_f = \mathrm{P}\{g(\mathbf{X}) \leq 0\}$, in which $g(\mathbf{X})$ is the so-called limit state function and $\mathbf{X}$ represents the vector of random variables. Usually, structural codes determine the required reliability of the structure with a target reliability index β_T, which relates to the failure probability by $P_f = \Phi(-\beta_T)$, in which $\Phi()$ denotes the cumulative distribution function of the standardized normal distribution. In this study, γ_{ADM} is calibrated to fulfil the reliability requirements of Eurocode [8] which imposes $\beta_T = 3.8$ for 50 years reference period and reliability class 2 structures. The current Eurocode considers only structural members in the reliability differentiation, although GMNIA can be utilized for entire structural systems for which the desired value of the reliability index may differ from the ones given in the present Eurocode. Therefore, in addition to γ_{ADM}-values corresponding to $\beta_T = 3.8$, the γ_{ADM}-*values* are also studied for varying reliability index β.

This study adopts a two-step procedure in determining the γ_{ADM} -values [14]: (1) Statistical distributions of the resistance of trusses are determined by Monte Carlo simulations (MCS) in which loads are assumed deterministic [17]; (2) Subsequently, the distributions of resistance are combined with the distributions of loads by using the First-Order Reliability Method (FORM) [17] to obtain the required γ_{ADM} -values. In MCS, a total of 19 random variables contributing to the resistance (see Tables 1, 2, and 4, note that bow imperfections are in both directions) are considered. Latin hypercube sampling is employed to reduce the required number of samples. Sample size of $n_{MCS} = 500$ was selected for MCS based on a preliminary test made for K-truss with a 24 m span length: the distributions of resistance were determined for sample sizes of 60, 125, 250, 500 and 1000, and MCS with 250 samples converged already rather closely with distribution of 1000 samples.

In this study, Eurocode 0 [8] load combination 6.10 is considered for a single variable load. Based on Equation (1), the expression 6.10 yields:

$$\frac{R_n}{\gamma_{ADM}} \geq \gamma_G \bullet G_k + \gamma_Q \bullet Q_k = 1.35G_k + 1.5Q_k \tag{4}$$

in which G_k is the characteristic value of the permanent load and Q_k characteristic value of the variable load. Based on this equation, the following limit state function is considered which accounts for a random resistance R with a one random variable load Q in conjunction with a random permanent load G [38]:

$$g(\mathbf{X}) = R - G - Q \leq 0 \tag{5}$$

In FORM, only the relative magnitudes of nominal and characteristic values are important, not the actual magnitudes. The relative magnitudes are obtained by assuming that structures are designed economically at their limits, i.e. assuming that the design resistance equals the design loads in Equation (1). By introducing the term $\alpha_Q = Q_k/G_k$, which is the ratio of characteristic values of the variable to permanent load, the characteristic values for loads can then be obtained by [38]:

$$G_k = \frac{R_n/\gamma_{ADM}}{\gamma_G + \gamma_Q \alpha_Q}$$

$$Q_k = \frac{\alpha_Q R_n/\gamma_{ADM}}{\gamma_G + \gamma_Q \alpha_Q} \tag{6}$$

in which the substituted partial factors are $\gamma_G = 1.35$ and $\gamma_Q = 1.5$, see Eq. (4). In the limit state function of Equation (5), random variables are modelled according to their statistical properties, which are presented in Table 9. For the resistance, statistics must be determined individually for every structure by MCS. This involves the determination of the distribution type, mean-to-nominal ratio $R_{MtoN} = mean(R_i)/R_n$, and coefficient of variation (CoV) for relative resistances R_i/R_n, in which $i = 1 \ldots n_{MCS}$, R_i is the capacity of the i:th sample in MCS and R_n is the nominal capacity, i.e. the lowest capacity obtained among the nominal models. Reliability indexes β can then be derived by FORM for a given range of γ_{ADM}-values.

Permanent loads presented in Table 9 consider the self-weight of steel structures and self-weights of non-structural elements, such as insulated roof panels for example. Although the snow load is usually the most governing load for roof trusses at least in the Nordic countries, and the truss configurations of this study were originally determined based on the magnitude of snow load, imposed and wind loads are additionally considered in the reliability studies to cover a wider range of truss applications and to obtain comparable safety factors with other studies. The limit state function in Equation (5) is studied individually for every variable load such that Q and Q_k represent a random variable and characteristic value of imposed, snow and wind load one at a time.

Varying α_Q-values must be considered in FORM to cover the whole meaningful design spectrum. Additionally, weights w for α_Q-values are usually determined such that some design cases are considered more important than others. For the target reliability index $\beta_T = 3.8$, the safety factor γ_{ADM} is determined by minimizing the weighted least-squares error $S = \sum_{i=1}^{5} (\beta_T - \beta_i)^2 \bullet w_i$, where β_i is the nominal reliability index of case i [17,39]. The $\alpha_{Q,i} - (w_i)$ value-pairs for the cases i are assumed as 1.0 (6 %), 1.5 (17 %), 2.0 (22 %), 3.0 (33 %) and 5.0 (22 %). These value-pairs were estimated to be suitable for steel structures in other studies [40,5].

7. Reliability studies of K-trusses

In the following subsections, the results of nominal analyses and MCS are first presented. These are essential ingredients in FORM, allowing for the determination of the mean-to-nominal ratios and CoVs for the resistance. Subsequently, the statistics of resistance are combined with

Table 9
Probabilistic models of the resistance and loads.

Property	Description	Distribution	Mean and CoV	Char. val.	Ref.
R	Resistance	Lognormal	$\mu = R_{MtoN} \bullet R_n$, CoV of R_{MtoN}, see Table 10	R_n	MCS
G	Permanent load	Normal	$\mu = G_k$, CoV = 0.1	G_k	[41]
$Q_{Imp,50}$	Imposed load, 50 years	Gumbel	$\mu = 0.6Q_{k,Imp,50}$, CoV = 0.35	$Q_{k,Imp,50}$	[41]
$Q_{wind,50}$	Wind load, 50 years	Gumbel	$\mu = 0.7Q_{k,wind,50}$, CoV = 0.35	$Q_{k,wind,50}$	[41]
$Q_{snow,50}$	Snow load, 50 years	Gumbel	$\mu = 1.0Q_{k,snow,50}$, CoV = 0.22	$Q_{k,snow,50}$	[42]

Table 10
Statistics for the resistance of trusses.

Truss	R_{MtoN}	CoV of R_{MtoN} [%]	R_n	Max. of $R_{n,i}$	CoV of $R_{n,i}$ [%]	$R_{n\pm}/R_n$
K12mF1	1.09	5.60	1.21	1.23	0.26	1.00
K12mF2	1.09	5.50	1.24	1.25	0.09	1.00
K12mF3	1.08	5.57	1.62	1.63	0.12	1.00
K12mF4	1.10	5.54	1.17	1.19	0.27	1.00
K12mF5	1.06	6.09	1.57	1.63	1.44	1.00
K24mF1	1.07	5.60	1.14	1.15	0.08	1.00
K24mF2	1.08	5.73	1.15	1.15	0.07	1.00
K24mF3	1.15	5.92	1.32	1.53	4.04	1.11
K24mF4	1.08	5.58	1.29	1.31	0.25	1.00
K24mF5	1.08	6.78	1.27	1.32	0.77	1.01
K48mF1	1.09	5.24	1.09	1.11	0.49	1.01
K48mF2	1.07	5.59	1.19	1.19	0.05	1.00
K48mF3	1.11	7.03	1.24	1.38	2.73	1.07
K48mF4	1.07	5.40	1.12	1.13	0.19	1.00
K48mF5	1.09	6.70	1.14	1.18	0.81	1.00

the variability of loads by FORM, providing the needed system safety factors γ_{ADM}.

7.1. Nominal capacity

Table 10 presents nominal capacities R_n in terms of the ultimate load factor α_u. Additionally, the maximum capacity Max $R_{n,i}$ and CoV for every 66 nominal analyses are presented in the table to illustrate the range of variation of the capacity in nominal models. The Max $R_{n,i}$ is close to R_n and CoV is below 1 %, i.e. relatively small, for every other analysis except for K12mF5, K24mF3, and K48mF3. This indicates that in most cases, the capacity of the truss is not sensitive to the assumed imperfection direction.

Table 10 also presents the ratio $R_{n\pm}/R_n$, and the difference is 1 % or less for every other case except for K24mF3 and K48mF3, in which the ratios are as high as 1.11 and 1.07, respectively. The sensitivity to imperfection directions is expectable in these cases because the failing members are the continuous top chords. In tensile members or compressed but pinned braces, it is natural that the sensitivity is much lower. In the case K12mF3, the failure mode was top chord yielding combined with the tensile fracture in the bottom chord, hence statistics of K12mF3 differ from K24mF3 and K48mF3 in Table 10.

No remarkable difference was obtained between resistances $R_{n\pm}$ in positive and negative directions, they vary less than 0.5 % for every other case except for K24mF3, in which the difference was 2 % in XZ-plane. Regarding the capacity $R_{n\pm}$ between XZ, YZ and 3D planes, nominal capacities were also very identical, probably because only a few rectangular sections were used and only in compression braces near mid-span, in which the utilization ratios were low.

Although top chords are sensitive to imperfection directions, the results above indicate that in most cases, the nominal capacity is rather accurately obtained by analyzing only a single nominal model with positive imperfection direction in every member. Consequently, in the GMNIA process, it is computationally efficient to use only a single nominal model in the iteration phase when searching for suitable cross-sections and perform a more comprehensive investigation using multiple nominal models once a sophisticated guess of the final configuration is obtained.

Table 10 shows a trend that, on average, nominal capacities R_n are decreasing with increasing span length. For example, K12mF1 has 6 % and 11 % higher nominal capacity than K24mF1 and K48mF1, respectively. This trend is probably caused by the inclusion of the corner strength enhancement to the model (see Section 2): cross-sections with a small width-to-thickness ratio have a larger proportion of corner material than wider and thinner sections, and trusses with short span lengths consist mostly of small cross-sections. However, this feature does not affect the reliability studies, because applied loads in FORM are relative to nominal resistances, see Eq. (6).

7.2. Statistics for the resistance

Table 10 presents mean-to-nominal ratios R_{MtoN} and their CoVs obtained from MCS. Mean-to-nominal ratios vary in the range of 1.06–1.15 and CoVs in the range of 5–7 %. CoVs are small when compared to cold-formed steel and stainless steel framed structures, in which CoVs of 7–12 % have been reported [5,38]. However, similarly small CoVs, ranging from 4 to 9 %, have been observed for roof trusses [43].

Statistics for R_{MtoN} in Table 10 already contain the effects of modelling uncertainty θ_M (see Table 4). Modelling uncertainty was considered by multiplying the randomly generated θ_M -values with the resistances obtained from MCS. It is worth mentioning that before the application of θ_M, resistances of cases K12mF5, K48mF3 and K48mF4 resembled Weibull distribution, whereas other cases Lognormal distribution. Lognormal distribution is typically assumed for resistances of steel structures [5,15,38,44], but additionally, Weibull distributions can be observed in "weakest link" structural systems [25]. After considering θ_M, the product distributions for the resistance followed thoroughly Lognormal distribution for every other case except for K24mF2 and K48mF3. Lognormal assumptions were verified by visual comparison of data to probability plots, probability density functions (PDF) and cumulative distribution functions (CDF). Additionally, Anderson-Darling goodness-of-fit tests with a 5 % significance level [45] were employed. Fig. 7 presents the histogram, PDF and CDF for the case K12mF1. Fitted Lognormal distribution follows closely histogram and Empirical CDF. Fig. 8 presents the histogram, PDF and CDF for the case K24mF2, in which the null hypothesis was rejected by the Anderson-Darling test with a p-value of 4.6 %. The lognormal distribution gives still a rather good fit and is therefore chosen. K48mF3 was also rejected by the Anderson-Darling test and Fig. 9 presents both Lognormal and Weibull distributions for the case because the resistance followed Weibull before the application of θ_M. Lognormal seems to have slightly better fit to data and is therefore chosen for K48mF3. Consequently, Lognormal distributions are assumed for the resistances of every truss.

7.3. System safety factor γ_{ADM}

Table 11 presents the results of FORM for γ_{ADM} -values corresponding to the target reliability index $\beta_T = 3.8$. The needed average γ_{ADM} is 1.13, 1.28 and 1.35 when assuming that the variable load is imposed, wind and snow, respectively. Snow requires much greater γ_{ADM} than imposed or wind load because the statistical distribution for snow is much more demanding. According to Table 9, the mean snow load equals the characteristic snow load during the 50-year return period, hence there is no intrinsic safety in the characteristic value of snow load. By contrast, the mean imposed load is only 60 % of the characteristic value, albeit CoV is higher than for snow.

Table 11 presents also weighted average γ_{ADM}-values "33-33-33" and

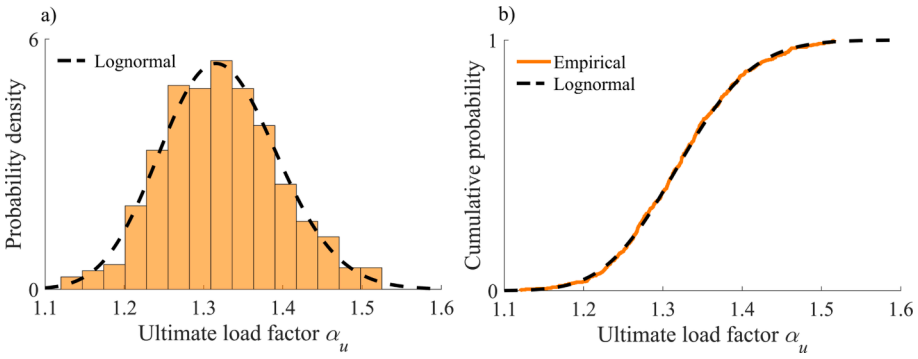

Fig. 7. PDF (a) and CDF (b) of the case K12mF1.

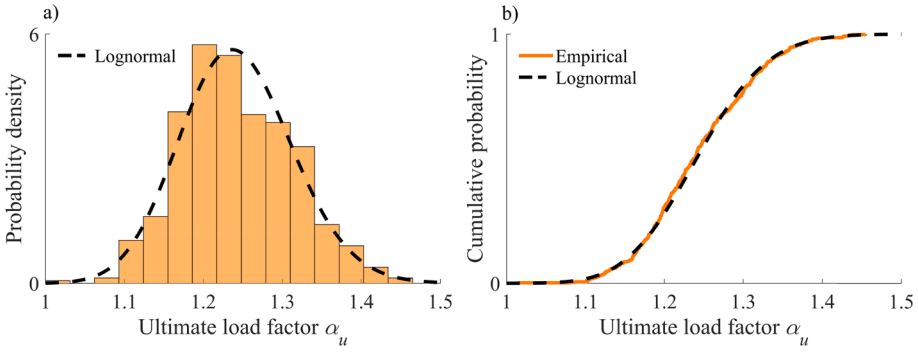

Fig. 8. PDF (a) and CDF (b) of the case K24mF2.

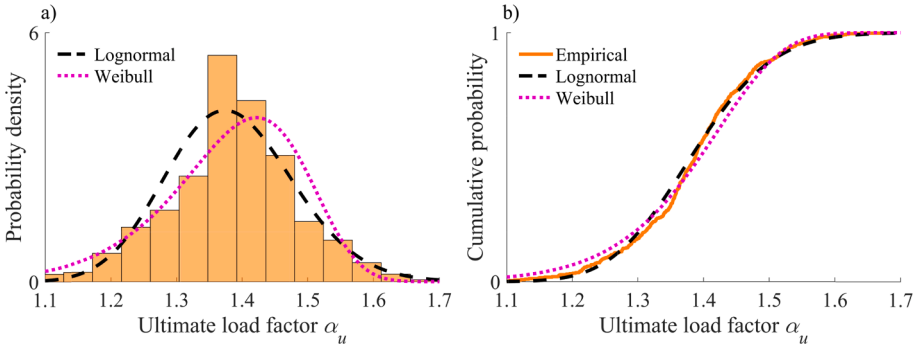

Fig. 9. PDF (a) and CDF (b) of the case K48mF3.

"50-40-10", the former having even weight, 33.3 %, for every load and the latter 50 % for imposed, 40 % for wind and 10 % for snow as suggested in [39]. Giving only a 10 % weight for snow load leads to a much lower average safety factor than the snow load would require for $\beta_T = 3.8$. In general, rather uniform γ_{ADM} -values are obtained regardless of failure mode or span length for a given load combination (see each column of Table 11), except in case K24mF3, which requires much lower γ_{ADM} due to higher mean-to-nominal ratio (see Table 10). Therefore, it is possible to select a single γ_{ADM} to be used for various trusses and failure modes and still have an acceptable low variation of the reliability level among the designed systems.

Fig. 10 depicts $\gamma_{ADM} - \beta$ diagrams for cases K12mF1, K12mF5, K24mF3 and K48mF2, which have the most dissimilar γ_{ADM} -values among the studied cases. The diagrams present $\gamma_{ADM} - \beta$ values for every load and α_Q-ratio. In these diagrams, the uppermost curves in imposed, wind and snow loads correspond to $\alpha_Q = 1$, the next highest to $\alpha_Q = 1.5$, etc., and the lowest curves correspond to $\alpha_Q = 5$, see Fig. 10 (a). This is because the variability in variable loads is much greater than in permanent load, hence increase in the α_Q-ratio decreases the reliability index for the fixed γ_{ADM}. Based on these diagrams, γ_{ADM} can be determined for varying target reliability index β_T.

Table 11
γ_{ADM} -values for $\beta_T = 3.8$.

Truss	$G + Q_{Imp,50}$	$G + Q_{Wind,50}$	$G + Q_{Snow,50}$	Weighted 33–33–33[1]	Weighted 50–40-10[2]
K12mF1	1.13	1.28	1.34	1.25	1.21
K12mF2	1.13	1.28	1.34	1.25	1.21
K12mF3	1.14	1.29	1.35	1.26	1.22
K12mF4	1.12	1.27	1.33	1.24	1.20
K12mF5	1.16	1.32	1.39	1.29	1.25
K24mF1	1.14	1.30	1.36	1.27	1.23
K24mF2	1.13	1.29	1.35	1.26	1.22
K24mF3	1.07	1.21	1.27	1.18	1.15
K24mF4	1.14	1.29	1.35	1.26	1.22
K24mF5	1.15	1.30	1.37	1.27	1.23
K48mF1	1.12	1.27	1.33	1.24	1.20
K48mF2	1.15	1.30	1.37	1.27	1.23
K48mF3	1.12	1.27	1.33	1.24	1.20
K48mF4	1.14	1.30	1.36	1.27	1.23
K48mF5	1.14	1.29	1.36	1.26	1.22
Average	1.13	1.28	1.35	1.25	1.21

[1] Average, i.e. even weights for imposed, wind and snow load.
[2] Average by giving 50 %, 40 % and 10 % weights for imposed, wind and snow load, respectively.

8. Comparing GMNIA with conventional design approach

According to Table 11, the system safety factor for the weighted average "50-40-10" was $\gamma_{ADM} = 1.21$. This safety factor is now employed for comparison calculations, in which three K-trusses are designed according to both the conventional EN 1993-1-1 method and GMNIA. Designed trusses are K30m, K35m and K40m, and their layouts are presented in Table 12 and Fig. 11. Design principles, including loads and boundary conditions, are the same as presented in Section 3, except that in addition to reduced buckling lengths of top chords, the buckling lengths of braces are reduced by the factor of 0.75 as allowed for welded hollow section connections [1]. The aim is to obtain minimum weight truss configurations for both methods.

Design forces for the conventional method were determined by geometrically nonlinear elastic analysis (GNA) considering second-order effects. Comparisons to geometrically linear analyses showed that the second-order effects affected significantly only the bending moments of top chords, increasing them by at most 20 % from moments obtained by linear analysis. For the centermost braces B7 and B8 shown in Fig. 11, second-order effects increased axial forces up to 50 %, but this had an insignificant effect because the centermost braces had only minor axial forces and low utilization ratios such that the absolute increase in the magnitude due to second-order effects was rather negligible. For all other members, design forces obtained by geometrically linear and nonlinear analyses differed at most by only few percent. It should be noted that for K35m and K40m with pinned connections in GNA, critical braces buckled before the design load was reached. Therefore, for K35m and K40m, GNA was exceptionally carried out by assuming rigid connections in braces. For K30m, however, GNA was successfully carried out twice (with pinned and fixed connections), and no remarkable differences were obtained between the design forces.

Table 13 presents the designed configurations for the conventional method (Conv.) and GMNIA. The naming convention of truss members is shown in Fig. 11, brace B1 being the outermost brace and B8 the centermost. Configurations for GMNIA have been obtained by trial and error, without any automated optimization algorithm. GMNIA results in 4.2 % and 0.2 % heavier trusses for K30m and K40m, respectively. For K35m, however, GMNIA yields a 1.4 % lighter truss. It was found that GMNIA allows for lighter top chords in general (see, e.g. K35m and K40m in Table 13), but on the contrary, it requires heavier compression braces and tensile members than the conventional method.

In the case of the top chord, GMNIA can more accurately consider the continuity of the chord than the conventional method which must rely on the approximation that the buckling length of the chord is 0.9 times the system length. It has been shown in the literature that the real buckling length reduction factors of chords vary in the range of 0.6–0.9 [46,47], but to facilitate design based on elastic analysis a conservative value 0.9 is employed. Therefore, the accuracy of GMNIA may provide substantial material savings such as in the case of K35m, in which the mass of the top chord comprises about 60 % of the total mass of the truss, and GMNIA results in even 10 % lighter top chord than the conventional design approach.

In the case of compression braces (B2, B4, B6 and B7), however,

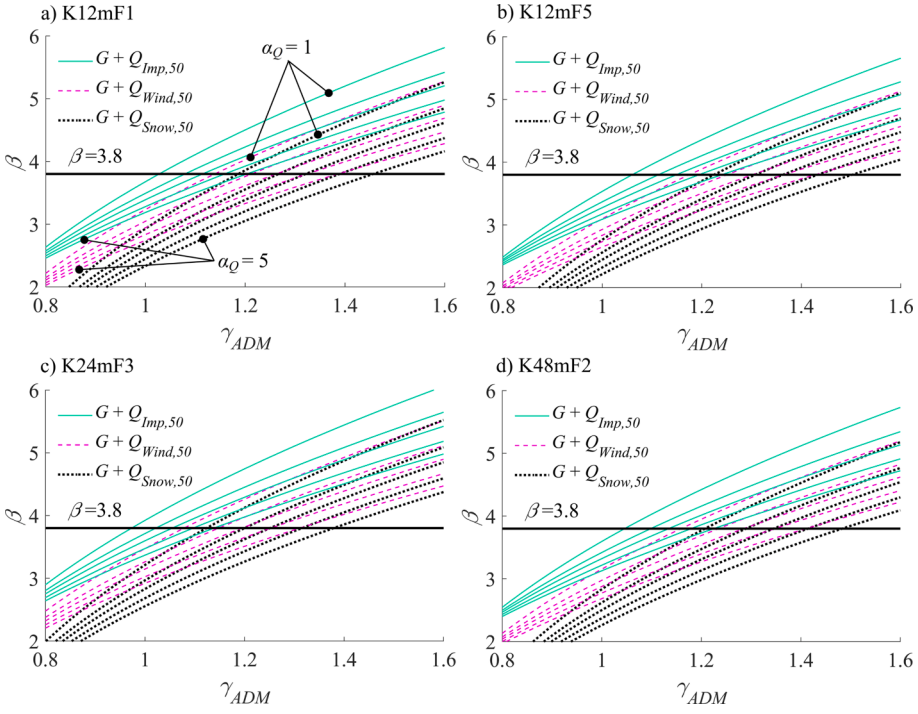

Fig. 10. $\gamma_{ADM} - \beta$ diagrams for selected cases.

Table 12
Base geometries of trusses K30m, K35m and K40m.

Truss	L_s [m]	H_s [m]	H_m [m]	Num. of braces	TC_1; TC_2; TC_3; TC_4 [m]	BC_1; BC_2; BC_3; BC_4 [m]
K30m	30	2.06	3.00	16	4.1; 3.4; 3.7; 3.9	3.7; 3.4; 4.0; 1.7
K35m	35	2.41	3.50	16	4.6; 4.1; 4.3; 4.5	4.3; 3.9; 4.7; 2.0
K40m	40	2.75	4.00	16	5.3; 4.6; 4.9; 5.1	5.0; 4.5; 5.3; 2.3

GMNIA results in significantly larger cross-sections than the conventional design approach. Two reasons can explain this. Firstly, conventional method utilizes the buckling length reduction by a factor of 0.75, whereas GMNIA assumes pinned connections for braces. Therefore, GMNIA is inferior in the buckling capacity of braces, and the connection stiffness should be accounted for in GMNIA. The component method [48] offers a solution for incorporating the connection stiffness in ADM as systems of springs. Unfortunately, the component method has not yet been developed for K-joints of CFRHS in NFEM.

Secondly, larger compression braces probably result from the somewhat conservative value for the system safety factor, namely $\gamma_{ADM} = 1.21$. It was observed during the design by GMNIA procedure that in some cases GMNIA resulted in larger compression braces than the conventional method even without buckling length reduction. Additionally, GMNIA is inferior also in the bottom chord of K35m and K40m, and brace B3 of K40m. Bottom chords are about 8–9 % heavier in GMNIA. The tensile strength in the conventional method is obtained by $N_{t,Rd} = Af_y/\gamma_{M0}$, in which A is the cross-sectional area, f_y the nominal yield stress 700 MPa, and partial factor $\gamma_{M0} = 1.0$ [1]. GMNIA, which utilizes the effective material model [10], has the same cross-sectional area as the conventional method. However, the EMM considers the strain hardening such that the tensile resistance is determined based on the ultimate stress f_u. For a bottom chord of 50×120×6 in K40m, about 55 % of the total cross-sectional area is assumed to consist of corner material because of the extended distance 2 times the wall thickness from the corner to the flat region (see Fig. 3). The nominal f_u for the flat material is 750 MPa and for the corner material 870 MPa ($C_{fu} = 1.16$, see Table 2). Consequently, the f_u in EMM is 750 MPa•(1–0.55) + 870 MPa•0.55 = 816 MPa. The ratio of the tensile strengths employed, 816 MPa/700 MPa = 1.17, corresponds to the ratio of tension resistances of the cross-section in GMNIA and in conventional method. Therefore, if $\gamma_{ADM} > 1.17$, the tension resistance of the section 50×120×6 is less efficient in GMNIA than in the conventional method because the loads of conventional method, and almost proportionally the load effects in case of minor load redistribution, are multiplied by the factor of γ_{ADM} in GMNIA.

Similar indication about the over-conservativity regarding $\gamma_{ADM} = 1.21$ is obtained by inspecting nominal resistance of cases K12mF1, K24mF1 and K48mF1 (see Table 10). These cases were designed by the conventional method with a target utilization ratio of 100 % for each member and without buckling length reduction for braces, hence being comparable to pinned GMNIA design. The average nominal resistance for these cases is only 1.15, i.e. remarkably lower than 1.21 which would be required.

The value of $\gamma_{ADM} = 1.21$ was determined based on the target reliability index of $\beta_T = 3.8$, which is the required reliability index for structural members in Eurocode 0 [8]. The load redistribution capability and redundancy are very limited in the investigated trusses such that

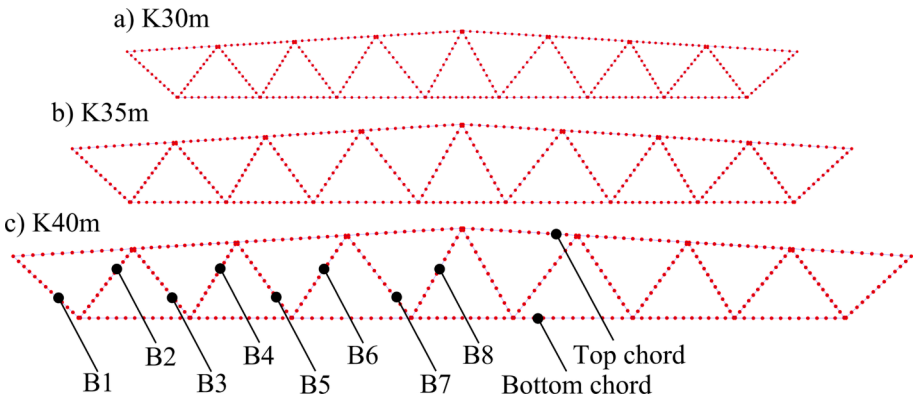

Fig. 11. Geometries and FEM meshes of trusses K30m, K35m and K40m.

Table 13
Truss configurations designed by conventional method and GMNIA with $\gamma_{ADM} = 1.21$.

Member	K30m		K35m		K40m	
	Conv.	GMNIA	Conv.	GMNIA	Conv.	GMNIA
Top chord	150×150×6	150×150×6	180×120×8	180×120×7.1	200×120×8.8	200×120×8
Bot. chord	50×100×5	50×100×5	80×120×4	60×120×5	60×100×6	50×120×6
Brace B1	60×60×3	60×60×3	70×70×3	70×70×3	70×70×4	70×70×4
Brace B2	90×90×4	100×100×5	90×90×5	110×110×5	100×100×6	120×120×6
Brace B3	30×40×3	30×40×3	40×40×3	40×40×3	40×40×3	40×40×4
Brace B4	70×70×4	90×90×4	80×80×4	100×100×4	90×90×4	110×110×5
Brace B5	25×25×3	25×25×3	25×25×3	25×25×3	25×25×3	25×25×3
Brace B6	70×70×3	80×80×4	70×70×4	90×90×4	80×80×4	100×100×4
Brace B7	50×50×3	50×50×3	50×50×3	60×60×3	80×80×4	80×80×4
Brace B8	25×25×3	25×25×3	25×25×3	25×25×3	25×25×3	25×25×3
Total mass	1305 kg	1360 kg	1872 kg	1845 kg	2532 kg	2536 kg

these structures can be considered as weakest link models or series systems. Eurocode does not yet consider target reliability requirements for structural systems. For weakest link models, however, a lower reliability index could be justified. Assume for example, that members which have over 98 % utilization ratio in the conventional method are at significant risk of failure. Trusses K30m, K35m and K40m contain 1 (TC), 2 (BC, B2) and 3 (TC, BC, B3) members which exceed this threshold, respectively. Thus, on average, these trusses have a total of 4 members at significant risk of failure (2 members on each side of the apex). Assuming that a failure in a single member leads to the failure of the whole truss and that failures of these members are mutually exclusive events, the probability of failure of the conventionally designed truss is $P_f = 4 \bullet \Phi(-3.8) = 2.89\text{e-}4$ [17], resulting to a reliability index of 3.44. If the target reliability index 3.44 is selected instead of 3.8 for system level reliability differentiation in Section 7.3, the averaged safety factors reduce from 1.25 to 1.14 in weighting 33-33-33 and from 1.21 to 1.10 in 50-40-10 (see Table 11). Although the example above is highly simplified, it highlights how significantly the required system safety factor can decrease when studying reliability at the system level instead of member level.

Based on the $\gamma_{ADM} = 1.10$ and 1.14 obtained with $\beta_T = 3.44$ and additionally by considering the average nominal capacity 1.15 of trusses K12mF1, K24mF1 and K48mF1, the value $\gamma_{ADM} \approx 1.15$ seems suitable for the GMNIA of truss structures. Australian and New Zealand standard for cold-formed steel structures [13] suggests a capacity reduction factor of 0.85 for prequalified systems in ADM. The capacity reduction factor is used as a reciprocal for the γ_{ADM} leading to $\gamma_{ADM} \approx 1.18$. Arrayago and Rasmussen suggested $\gamma_{ADM} = 1.15$ for the Eurocode-based design of stainless steel frames under imposed loads, whereas the current study resulted in $\gamma_{ADM} = 1.13$ (average of imposed loads in Table 11). Although the Australian and New Zealand standard differs from Eurocode in codification, and the above-mentioned γ_{ADM} –values are based on various kinds of structural systems, the obtained system safety factors seem very similar. This implies that a wide variety of structural systems could be designed by using only a few system safety factors, which is a desired outcome regarding the simplicity of the GMNIA method.

9. Material efficiency in GMNIA trusses

In the literature, design by ADM has reduced the material consumption compared to conventional design methods: Ziemian analyzed planar [3] and 3D [4] frames made of American hot-rolled wide flange beams, and inelastic second-order analyses resulted in 12–13 % lighter structures than the conventional load and resistance factor design. Liu et al. [5] analyzed a CFRHS frame, and ADM resulted in a 14 % lighter structure than the conventional method. These frames were capable of redistributing loads through plastic hinges, unlike currently studied trusses in which load redistribution capabilities are very limited. The following three rough estimations are deduced from the compared truss designs of Table 13 regarding the material consumption in GMNIA:

1. GMNIA does not seem to offer any benefits if pinned connections are assumed between compression braces and chords. The reduced weight of the top chord is counteracted by heavier compression braces and tensile members such that the total mass becomes almost equal in GMNIA and the conventional method.
2. GMNIA can achieve about 5 % reduction in material consumption if stiffness of the brace connections can be considered in NFEM analysis (e.g. by the component method) and γ_{ADM} is not overconservative such that braces and bottom chord are identical in both methods. This is possible because the top chord is about 50–60 % of the total weight of the truss and GMNIA can offer even 10 % lighter top chord, hence $0.5 \bullet 0.1 = 5$ %.
3. Real buckling length reduction factors of braces vary in the range of 0.5–1.0 such that the constant factor 0.75 can be un- or overly conservative [46]. Compression braces and top chord comprise about 75 % of the weight of the trusses of Table 13. If similar 10 % material reduction is possible also in the compression braces as in the top chord, $0.1 \bullet 0.75 \approx 8$ % reduction in material consumption can be achieved by GMNIA. Naturally, this requires that brace connections can be accurately modelled in GMNIA without over-conservativity. No material reduction is expected regarding the tensile members.

The above estimations can vary substantially depending on how accurately connections of braces can be modelled and what the required reliability index for series systems is. It was observed by conducting the GMNIA design process of K40m for example, that by $\gamma_{ADM} = 1.13$ the top chord would have been 14 % lighter than in the conventional method, resulting in even $0.14 \bullet 0.75 \approx 11$ % reduction in material consumption according to Item 3 above. However, this amount of reduction in material consumption is probably an upper bound, and the expected realistic range is 5–8 %. Additionally, serviceability limit state requirements such as the maximum allowed deflection may require larger cross-sections than the ultimate limit state thus reducing the effectiveness of GMNIA in practical applications. On the other hand, it is worth reminding that the potential material reduction is not the only benefit that ADMs can offer. From the viewpoint of structural safety, a comprehensive understanding of the collapse mode of the system and a uniform system reliability level are very valuable features that design by ADM provides [6].

10. Discussion and further research

A practical comparison in Section 8 indicated that $\gamma_{ADM} = 1.21$ leads to an overly conservative design compared to the conventional method, and $\gamma_{ADM} \approx 1.15$ could be more appropriate. On the other hand, trusses have considerably lower reliability indices for snow and wind loads than for imposed load as shown in Fig. 10, because snow and wind have more demanding probabilistic models (see Table 9). According to Table 11, the averaged γ_{ADM} is 1.35 for snow load, which would lead to an extremely conservative design compared to the conventional method. Similar observation was obtained for stainless steel frames against wind loads, in which an average system safety factor of 1.55 was derived with wind-to-dead load ratios ranging between 2.5 and 7.0 and for $\beta_T = 3.8$ [49]. If the trusses of the present study were resisting significant wind loads, corresponding system safety factor for wind would be ≈1.4 ($\beta_T = 3.8$, $\alpha_Q = 5$) according to Fig. 10 (a). Such a high variation in reliability level between loads is a remarkable issue because the design becomes very uneconomical if γ_{ADM} is chosen based on climatic loads only and, on the contrary, very unconservative if γ_{ADM} is selected based on averaging.

It must be highlighted that the suggested $\gamma_{ADM} \approx 1.15$ in this study is only a preliminary assumption for a suitable value of the system safety factor of CFRHS trusses made of steel grade S700. The following 5 issues should be solved before final decisions about γ_{ADM} can be made:

1. Probabilistic models and weight factors of loads have an enormous effect on the derived system safety factor. System safety factors may change after the publication of the reliability background of Eurocodes [39], when the commonly accepted models become available.
2. System-level target reliability is still an open issue in Eurocodes, and decisions are needed for the required target reliability index of various systems.
3. A modelling method for brace connections is needed if reduced material consumption is desired by GMNIA. Statistical properties of the truss resistance may change when considering the brace connections, thus affecting the derived system safety factors.
4. This study utilizes the effective material model, which considers the enhanced corner strength properties due to cold-forming. Although the accuracy of the EMM procedure has been validated [10], a considerable uncertainty exists regarding the corner strength enhancement factors which are based on only 12 measurements (see Table 2). To reduce this uncertainty and to fully exploit beneficial

strength enhancements due to cold-forming in the EMM, more experimental data should be analyzed.
5. Further studies are needed to cover a wider range of truss geometries and loading conditions, and additional steel grades, such that the design procedure can be widely adopted for various structural systems.

11. Conclusions

In this study, Monte Carlo simulations and reliability studies were carried out for 15 varying tubular high-strength steel roof trusses to determine the required system safety factor γ_{ADM} for the Eurocode-compliant GMNIA-procedure. For the Eurocode reliability index requirement of 3.8, derived system safety factor was $\gamma_{ADM} = 1.21$.

The comparison of three trusses designed by GMNIA with $\gamma_{ADM} = 1.21$ and by the conventional member-based EN 1993-1-1 approach illustrated that GMNIA resulted in 4.2 % and 0.2 % heavier, and 1.4 % lighter trusses than the conventional method. It was also shown that GMNIA enables lighter top chords because it accurately captures the buckling capacity of continuous chords, whereas the conventional method must rely on an approximated buckling length. For the compression braces and tensile members, however, GMNIA resulted in larger member profiles. Pinned connections for braces were assumed in GMNIA because a suitable modelling method for brace connections is not yet available, whereas conventional method utilized reduced buckling lengths [1]. Appropriate modelling of the brace connections, e.g. by the component method [48], may overcome this inefficiency.

The present study showed that the efficiency of design by GMNIA depends strongly on the target reliability index. The currently employed reliability index values of Eurocode 0 are based on design of individual members. For weakest link systems, such as the trusses of this study, lower reliability index may be justified. System-level reliability is still an open issue for most design codes, and requires further research and discussions within code committees.

If a lower target reliability index is allowed for truss structures, and if brace connection stiffness can be accurately accounted for in the computational model, it was estimated that about a 5–8 % reduction in material consumption can be achieved by using GMNIA in the ultimate limit state design. This observation highlights the importance of incorporating the behavior of connections in the structural analysis to obtain the most economical solutions in the system-level design approach.

CRediT authorship contribution statement

Lauri Jaamala: Conceptualization, Methodology, Software, Formal analysis, Investigation, Writing – original draft, Visualization. **Kristo Mela:** Resources, Software, Writing – original draft, Validation, Supervision, Project administration, Funding acquisition. **Juha Tulonen:** Data curation, Writing – review & editing. **Anssi Hyvärinen:** Data curation, Writing – review & editing.

Declaration of Competing Interest

The authors declare that they have no known competing financial interests or personal relationships that could have appeared to influence the work reported in this paper.

Data availability

Data will be made available on request.

Acknowledgements

This research was funded by the Doctoral School of Industry Innovations at Tampere University and SSAB. The funding and support are gratefully acknowledged.

References

[1] EN 1993-1-1. Eurocode 3. Design of steel structures, Part 1-1. General rules and rules for buildings. European standard; 2005.
[2] EN 1993-1-5. Eurocode 3. Design of steel structures, Part 1-5. Plated structural elements. European standard; 2006.
[3] Ziemian RD, McGuire W, Deierlein GG. Inelastic limit states design. Part I: planar frame studies. J Struct Eng 1992;118:2532–49. https://doi.org/10.1061/(ASCE)0733-9445(1992)118:9(2532).
[4] Ziemian RD, McGuire W, Dierlein GG. Inelastic limit states design Part II: three-dimensional frame study. J Struct Eng 1992;118:2550–68. https://doi.org/10.1061/(ASCE)0733-9445(1992)118:9(2550).
[5] Liu W, Zhang H, Rasmussen K. System reliability-based Direct Design Method for space frames with cold–formed steel hollow sections. Eng Struct 2018;166:79–92. https://doi.org/10.1016/j.engstruct.2018.03.062.
[6] Rasmussen KJR, Zhang H. 00.01: Future challenges and developments in the design of steel structures – an Australian perspective. Ce/Papers 2017;1:81–94. https://doi.org/10.1002/cepa.75.
[7] EN 1991-1-1. Eurocode 1. Actions on structures, Part 1-1. General actions. Densities, self-weight, imposed loads for buildings. European standard; 2002.
[8] EN 1990. Eurocode 0. Basis of structural design. European standard; 2002.
[9] Ziemian RD. Guide to stability design criteria for metal structures. 6th ed. Hoboken, NJ: John Wiley & Sons; 2010.
[10] Jaamala L, Mela K, Tulonen J, Hyvärinen A. Effective material model for cold-formed rectangular hollow sections in beam element-based advanced analysis. J Constr Steel Res 2022;198. https://doi.org/10.1016/j.jcsr.2022.107569.
[11] prEN 1993-1-14. Eurocode 3. Design of steel structures. Part 1-14, Design assisted by finite element analysis. CEN/TC 250/SC 3 N 3653. European Committee for Standardization; 2022.
[12] Sun M, Packer JA. Direct-formed and continuous-formed rectangular hollow sections — comparison of static properties. J Constr Steel Res 2014;92:67–78. https://doi.org/10.1016/j.jcsr.2013.09.013.
[13] AS/NZS 4600. Cold-formed steel structures. Australian/New Zealand Standard; 2018.
[14] Zhang H, Shayan S, Rasmussen KJR, Ellingwood BR. System-based design of planar steel frames, I: reliability framework. J Constr Steel Res 2016;123:135–43. https://doi.org/10.1016/j.jcsr.2016.05.004.
[15] Zhang H, Shayan S, Rasmussen KJR, Ellingwood BR. System-based design of planar steel frames, II: Reliability results and design recommendations. J Constr Steel Res 2016;123:154–61. https://doi.org/10.1016/j.jcsr.2016.05.005.
[16] Zhang H, Ellingwood BR, Rasmussen KJR. System reliabilities in steel structural frame design by inelastic analysis. Eng Struct 2014;81:341–8. https://doi.org/10.1016/j.engstruct.2014.10.003.
[17] Melchers RE, Beck AT. Structural reliability analysis and prediction. 3rd ed. Hoboken, NJ: Wiley; 2018.
[18] Jaamala L, Mela K, Laurila J, Rinne M, Peura P. Probabilistic modelling of residual stresses in cold-formed rectangular hollow sections. J Constr Steel Res 2022;189:107108. https://doi.org/10.1016/j.jcsr.2021.107108.
[19] Shi G, Zhu X, Ban H. Material properties and partial factors for resistance of high-strength steels in China. J Constr Steel Res 2016;121:65–79. https://doi.org/10.1016/j.jcsr.2016.01.012.
[20] Gardner L, Nethercot DA. Numerical modeling of stainless steel structural components-a consistent approach. J Struct Eng (NY) 2004;130:1586–601. https://doi.org/10.1061/(ASCE)0733-9445(2004)130:10(1586).
[21] Cruise RB, Gardner L. Strength enhancements induced during cold forming of stainless steel sections. J Constr Steel Res 2008;64:1310–6. https://doi.org/10.1016/j.jcsr.2008.04.014.
[22] Ma J-L, Chan T-M, Young B. Experimental investigation on stub-column behavior of cold-formed high-strength steel tubular sections. J Struct Eng (NY) 2016;142:4015174. https://doi.org/10.1061/(ASCE)ST.1943-541X.0001456.
[23] Ma J-L, Chan T-M, Young B. Cold-formed high strength steel tubular beam-columns. Eng Struct 2021;230:111618. https://doi.org/10.1016/j.engstruct.2020.111618.
[24] Meng X, Gardner L. Behavior and design of normal- and high-strength steel SHS and RHS columns. J Struct Eng (NY) 2020;146:4020227. https://doi.org/10.1061/(ASCE)ST.1943-541X.0002728.
[25] Probabilistic model code. 12th draft. Joint Comittee on Structural Safety; 2001.
[26] prEN 1993-1-1. Eurocode 3. Design of steel structures, Part 1-1. General rules and rules for buildings. CEN/TC 250/SC 3 N 3159; 2020.
[27] Gardner L, Yun X. Description of stress-strain curves for cold-formed steels. Constr Build Mater 2018;189:527–38. https://doi.org/10.1016/j.conbuildmat.2018.08.195.
[28] Somodi B, Kövesdi B. RUOSTE - rules on high strength steel, deliverable 2.3. Global buckling tests; 2016.
[29] Suikkanen J. Compression tests of Ruukki's double grade tubes. Finland: Lappeenranta University of Technology; 2014. Master's Thesis (in Finnish).
[30] Wardenier J, Packer JA, Zhao X-L, van der Vegte GJ. Hollow sections in structural applications, second edition. CIDECT; 2010.
[31] Ongelin P, Valkonen I. SSAB Domex Tube, structural hollow sections. EN 1993-Handbook 2016. SSAB Europe Oy; 2016.
[32] Abaqus 3DEXPERIENCE R2019x. Dassault Systemes Simulia Corp., Johnston, USA.
[33] Afshan S, Theofanous M, Wang J, Gkantou M, Gardner L. Testing, numerical simulation and design of prestressed high strength steel arched trusses. Eng Struct 2019;183:510–22. https://doi.org/10.1016/j.engstruct.2019.01.007.
[34] EN 1993-1-12. Eurocode 3. Design of steel structures, Part 1-12. Additional rules for the extension of EN 1993 up to steel grades S 700. European standard; 2007.

[35] Shayan S, Rasmussen KJR, Zhang H. On the modelling of initial geometric imperfections of steel frames in advanced analysis. J Constr Steel Res 2014;98:167–77. https://doi.org/10.1016/j.jcsr.2014.02.016.
[36] Arrayago I, Rasmussen KJR. Influence of the imperfection direction on the ultimate response of steel frames in advanced analysis. J Constr Steel Res 2022;190:107137. https://doi.org/10.1016/j.jcsr.2022.107137.
[37] Beer H, Schulz G. The European column curves. IABSE reports of the working commissions; 1975.
[38] Arrayago I, Rasmussen KJR. System-based reliability analysis of stainless steel frames under gravity loads. Eng Struct 2021;231:111775. https://doi.org/10.1016/j.engstruct.2020.111775.
[39] Draft JRCreport - Reliability background in the Eurocodes - 2022-02-11. CEN/TC 250/SC 10 N 553; 2022.
[40] Ellingwood B, MacGregor JG, Galambos TV, Cornell CA. Probability based load criteria: load factors and load combinations. J Struct Div 1982;108:978–97. https://doi.org/10.1061/JSDEAG.0005959.
[41] Moore J. Safety of structures, an independent technical expert review of partial factors for actions and load combinations in EN 1990 "Basis of structural design; 2003.
[42] Holicky M. Safety design of lightweight roofs exposed to snow load. WIT Transactions on Engineering Sciences, Vol. 58, Southampton: WIT; 2007. p. 51–7. doi: 10.2495/EN070061.
[43] Blum H. Reliability-based design of truss structures by advanced analysis, Research report R936. School of Civil Engineering, The University of Sydney; 2013.
[44] Gulvanessian H, Holický M. Reliability based calibration of Eurocodes considering a steel member. JCSS workshop on reliability based code calibration; 2002.
[45] Dodge Yadolah. The concise encyclopedia of statistics. 1st ed. New York, NY: Springer New York; 2008. doi: 10.1007/978-0-387-32833-1.
[46] Boel H. Buckling length factors of hollow section members in lattice girders. Netherlands: Eindhoven University of Technology; 2010 (Master's Thesis).
[47] Haakana Ä. In-plane buckling and semi-rigid joints of tubular high strength steel trusses. Finland: Tampere University of Technology; 2014 (Master's Thesis).
[48] Yan S, Rasmussen KJR. Generalised Component Method-based finite element analysis of steel frames. J Constr Steel Res 2021;187:106949. https://doi.org/10.1016/j.jcsr.2021.106949.
[49] Arrayago I, Rasmussen KJR, Zhang H. System-based reliability analysis of stainless steel frames subjected to gravity and wind loads. Struct Saf 2022;97:102211. https://doi.org/10.1016/j.strusafe.2022.102211.